Journal of Academic Research Vol 30, Issu 02, 2026 "160-172"

Muti-Response Performance Optimization in the Turning Process of Low-Carbon Steel Alloys Using Response Surface Methodology and Desirability Function Approach

Mustafa Hakoumah[1], Salem Beleid[1], Abubkr Hemer[2], Benur Matug[3], Abdelnasir Shtewi[4]

[1]Al Asmarya Islamic University, Mechanical and Industrial Engineering Department, Libya
[2]Higher Institute of Engineering Technology, Zliten, Mechanical Engineering Department, Libya
[3]Almergib University, Mechanical Engineering Department, Libya
[4]Libyan Authority for Scientific Research, Libya

. **DOI:** https://doi.org/10.65540/hfqpts81

Article information **Abstract**

Key words
Surface Roughness, Material Removal Rate, Cutting Parameters, Surface Response, ANOVA.

Received 17 07 2026, Accepted 26 08 2026, Available online 29 08 2026

In the present investigation, Response Surface Methodology (RSM) in conjunction with the Desirability Function Approach (DFA) was utilized to ascertain the optimal values for cutting parameters—namely, cutting speed, feed rate, and depth of cut—with the objective of minimizing surface roughness and maximizing the Material Removal Rate (MRR). A Face-Centered Central Composite Design (FCCD) was implemented to systematically and effectively facilitate the experimental procedures. Second-order mathematical models for both MRR and surface roughness (Ra) were formulated based on the empirical data obtained from the experiments. The validity of these mathematical constructs was corroborated through (F-tests), and their adequacy was meticulously assessed utilizing Analysis of Variance (ANOVA) pertinent to the specified responses. Subsequently, the cutting parameters were optimized employing the predictive models generated through RSM, while a comprehensive multi-response optimization was executed via the desirability-based DFA. The findings indicated that the optimal values for the cutting parameters—resulting in the minimal surface roughness (1.8934 µm) and the maximal material removal rate (11,459 mm³/min)—were attained at a spindle speed of 1120 rpm, a feed rate of 0.20 mm/rev, and a depth of cut of 0.6788 mm. These results substantiate the efficacy of the proposed methodology in augmenting the machining performance of low-carbon steel alloys.

I. Introduction

The outcomes of metal machining operations are significantly influenced by input variables, as even minor fluctuations in these variables can result in substantial alterations in the resultant output variables. It is well-established that the surface integrity of a machined component profoundly affects its operational efficacy and longevity. The Material Removal Rate (MRR) in manufacturing represents a pivotal element due to its critical implications for industrial economic considerations. This reality has motivated numerous researchers and academic institutions to examine the effects of diverse input variables (including cutting parameters, tool

m.hakoma@asmarya.edu.ly

geometry, the characteristics and composition of workpiece materials, and the type of cutting fluid) on the quality of machined surfaces and their associated production costs, with the objective of optimizing these input variables to enhance output variables. This endeavor is supported by Design of Experiments (DOE) methodologies and various statistical techniques such as Response Surface Methodology (RSM), the Desirability Approach, the Taguchi Method, and Artificial Neural Networks, among others.

For instance, Abbas et al, [1] conducted a comprehensive investigation into the influence of cutting parameters on the AISI 1045 steel alloy, employing four distinct optimization algorithms, among which the WVGMO algorithm emerged as the most proficient in identifying optimal operational conditions.

Khan et al, [2] utilized the Taguchi method in conjunction with Response Surface Methodology to enhance turning performance, identifying the feed rate as the most significant variable, which culminated in a 30% reduction in tool wear and a 22% improvement in surface roughness.

Touggui et al, [3] implemented Response Surface Methodology alongside the Desirability Function to optimize the turning process of AISI 316L steel, resulting in an exceptional surface quality of 1.3 µm and a notable material removal rate of 12.346 cm^3/min.

Warsi et al, [4] ascertained the optimal machining parameters for Al 6061 T6 alloy through Grey Relational Analysis, achieving a 5% decrease in specific cutting energy and a 33% increase in material removal rate, while maintaining no significant variation in surface roughness.

Roy et al, [5] investigated the effects of cross-feed, workpiece velocity, cutting velocity, and depth of cut on interface temperature, material removal rate, and machining expenses during the face milling of AISI 4140 steel under both dry and wet conditions utilizing (RSM) and Design for Analysis (DFA). The optimal parameters were discerned, with wet conditions promoting temperature reduction and dry conditions demonstrating enhanced cost-efficiency attributable to the expenses associated with cutting fluids.

Zhang et al, [6] enhanced surface quality and material removal rate in the milling of short carbon fiber-reinforced PEEK composites through the application of (RSM) and Grey Relational Analysis. The optimal parameters (2600 rpm, 720 mm/min, 1.8 mm depth of cut) concurrently achieved minimal surface roughness and maximal material removal rate.

The objective of this study was to determine the optimal combination of machining parameters—namely cutting speed (v_c), feed rate (f), and depth of cut (a_p)—to simultaneously minimize surface roughness (Ra) and maximize the Material Removal Rate (MRR).

II. Research Methodology and Theoretical Framework

A. *Response Surface Methodology (RSM)*

Response Surface Methodology (RSM) is a robust statistical and mathematical technique utilized for modeling and analyzing engineering problems where the targeted response is influenced by multiple independent variables. This methodology relies on developing an empirical approximation model that correlates system inputs with outputs, predominantly employing a full quadratic regression model to capture non-linearities and curvature within the system. The general second-order polynomial equation is expressed as follows:

$$y = \beta_0 + \sum_{i=1}^{k} \beta_i x_i + \sum_{i=1}^{k} \beta_{ii}\ x_i^2 + \sum_{j \le i \le j}^{k} \beta_{ij} x_i x_j + € \qquad (1)$$

Where y represents the predicted response, x_i and x_j are the independent input variables, β_0 is the constant intercept, β_i denotes the linear effect coefficients, β_{ii} represents the quadratic effect coefficients, β_{ij} signifies the interaction coefficients between variables, k is the number of factors, and ε corresponds to the random experimental error.[7]

B. *Central Composite Design (CCD)*

Central Composite Design (CCD) matrices are widely employed to construct second-order response models with high computational efficiency. A standard CCD configuration consists of a k^2 factorial design augmented with center points and axial (star) points (α) to estimate process curvature Figure 1.

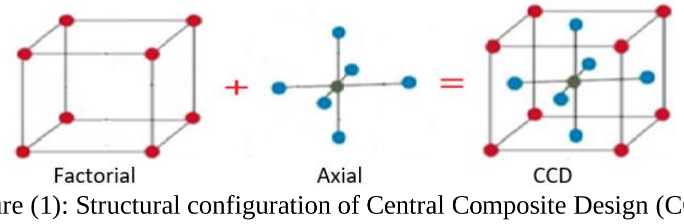

Figure (1): Structural configuration of Central Composite Design (CCD).

CCD variants are categorized based on the spatial location of the axial points:

- Circumscribed (CCC): The axial points are situated at a distance of (α) outside the factorial boundaries (α > 1), establishing spherical symmetry and requiring 5 factor levels.
- Face-Centered (CCF): The axial points are located at the center of each face of the factorial domain (α = ±1), requiring only 3 factor levels.
- Inscribed (CCI): Applied when factor bounds represent strict operational constraints, forming a scaled-down CCC design strictly within the specified limits using 5 factor levels

Alternatively, Box-Behnken Designs (BBD) are utilized as an economical alternative requiring fewer experimental runs. In BBD, design points are positioned at the midpoints of the process space edges, avoiding extreme factor level combinations [8] Figure 2.

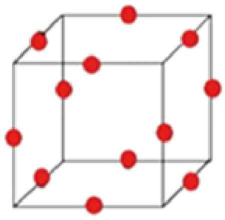

Figure (2): Structural configuration of Box-Behnken Design (BBD).

C. Multi-Response Optimization Using Desirability Function Approach (DFA)

The Desirability Function Approach (DFA) converts each measured response (Y_i) into an individual desirability value ($d_i(Y_i)$) ranging from 0 (a completely undesirable state) to 1 (the ideal response). The individual desirability functions are formulated based on the specific optimization objective (minimization, maximization, or achieving a target value) as follows [9]:

$$d_i(Y_i) = \begin{cases} 0, & Y_i < l_i, \\ \left(\dfrac{Y_i - l_i}{t_i - l_i}\right)^s, & l_i \le Y_i \le t_i, \\ \left(\dfrac{Y_i - u_i}{t_i - u_i}\right)^t, & t_i \le Y_i \le u_i, \\ 0, & Y_i > u_i, \end{cases} \quad (2)$$

Where l_i denotes the lower bound, u_i represents the upper bound, t_i signifies the target value, and s and t are weight exponents defining the functional shape of the desirability curve.
Subsequently, the individual desirability values are aggregated to calculate the overall composite desirability (D) using the geometric mean [10]:

$$D = \left(\prod_{i=1}^{n} d_i(Y_i)\right)^{\frac{1}{n}} \quad (3)$$

Where n represents the total number of target responses. Global multi-objective optimization is attained by maximizing D.

III. Experimental Procedures

A. Selection of Independent Variables and Process Levels

Based on preliminary brainstorming sessions, cause-and-effect (Ishikawa) diagrams, and a comprehensive literature review, three main cutting parameters were selected: rotational speed (N) feed rate (f), and depth of cut (a). Table 1 details these independent factors alongside their coded (-1, 0, +1) and actual (un-coded) physical levels.

Table (1): Cutting Parameters and Their Levels.

No.	Symbol	Factors /Variables	Levels		
1	N	Spindle Speed (Rev/min)	560	840	1120
2	f	Feed Rate (mm/rev)	0.1	0.15	0.2
3	a	Depth of Cut (mm)	0.4	0.6	0.8

B. Development of the Experimental Design Matrix

Minitab 18 software was utilized to generate the experimental design matrix governing the execution of the trials. The software provides various design matrix configurations tailored to the specified number of process factors and levels. Physical (actual) variables were transformed into coded dimensionless variables bounded within the range [-1, +1] using Equation (4):

$$x = \frac{x-\{x_{max}+x_{min}\}/2}{\{x_{max}+x_{min}\}/2} \tag{4}$$

Where X denotes the coded value of the variable, x represents the actual value of the process parameter, and x_{min} and x_{max} correspond to the minimum and maximum levels of the variable, respectively. The resulting experimental design matrix, generated according to the selected design methodology, is presented in Table 3, while the graphical representation of the design space is illustrated in Figure 3.

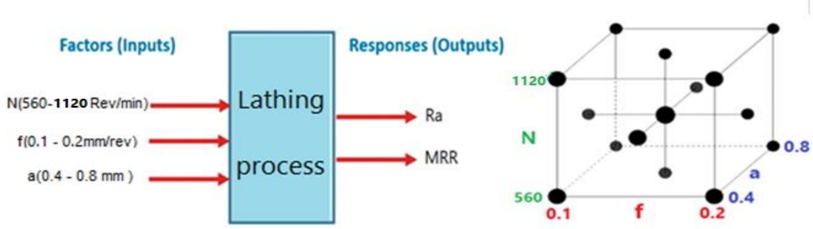

Figure (3): Layout of the Selected Design Matrix (Prepared by the Researcher).

C. Workpiece Material and Cutting Tool

Figures **4** and **5** illustrate the setup of the workpiece and cutting tool utilized in this study. Cylindrical specimens of **AISI 1018** steel with a diameter of **50** mm and a length of **110** mm were prepared on a conventional lathe (**AFM-TUG-40**) under dry cutting conditions using a carbide cutting tool.

Figure (4): Low-carbon steel alloy work piece.

Figure (5): Lathe machine used in the experiments.

Owing to its low carbon content (~0.18 wt%), AISI 1018 steel exhibits a predominantly ferritic-pearlitic microstructure, conferring high formability and weldability alongside moderate hardness. These physical and mechanical characteristics make AISI 1018 steel a standard reference material for investigating the effects of cutting parameters on machining forces, surface quality, tool wear, and Material Removal Rate (MRR), as well as evaluating the economic feasibility of the process. Table 2 outlines the specific chemical composition of the AISI 1018 steel alloy used in this study, derived from comparative gravimetric analysis.

Table (2): Chemical Composition of AISI 1018 Steel.

Fe	**S**	**P**	**Mn**	**C**	**Element**
Balance	≤0.050%	≤0.040%	0.60–0.90%	0.15–0.20%	AISI 1018

The experiments were conducted in accordance with the design matrix presented in Table 3, utilizing a Face-Centered Central Composite Design (CCF) configuration featuring six center points (**α = ± 1**). Additionally, the table details the measured values for average surface roughness (**Ra**) and Material Removal Rate (**MRR**) obtained across the various experimental runs.

Table (3): the experimental work and its results.

Run Order	Spindle Speed (Coded)	Feed Rate (Coded)	Depth of Cut (Coded)	Spindle Speed N (Rev/min)	Feed Rate f (mm/rev)	Depth of Cut a (mm)	Surface Roughness Ra (μm)	Material Removal Rate MRR (mm^3/min)
1	-1	1	-1	560	0.2	0.4	3.2	3460.53
2	-1	0	0	560	0.15	0.6	2.21	3861.45
3	0	0	0	840	0.15	0.6	2.21	5516.35
4	-1	1	1	560	0.2	0.8	3.14	6808.52
5	1	0	1	1120	0.1	0.8	1.75	6808.52
6	0	1	0	840	0.2	0.6	2.6	7355.14
7	0	0	-1	840	0.15	0.4	3.15	3707.71
8	1	1	1	1120	0.2	0.8	2.22	13617.04
9	0	0	0	840	0.15	0.6	2.21	5516.35
10	0	0	0	840	0.15	0.6	2.21	5516.35
11	0	-1	0	840	0.1	0.6	2.05	3677.57
12	1	0	0	1120	0.15	0.6	1.81	7722.89
13	0	0	0	840	0.15	0.6	2.21	5516.35
14	-1	-1	1	560	0.1	0.8	2.1	3404.26
15	-1	-1	-1	560	0.1	0.4	2.92	1730.27
16	0	0	1	840	0.15	0.8	2.85	7294.85
17	1	-1	-1	1120	0.1	0.4	2.12	3460.53
18	0	0	0	840	0.15	0.6	2.21	5516.35
19	1	1	-1	1120	0.2	0.4	2.64	6921.06
20	0	0	0	840	0.15	0.6	2.21	5516.35

IV. Results and Discussion

A. *Mathematical Model Development and Goodness-of-Fit Verification*

A second-order model was used to represent the output responses, namely (Ra) and (MRR). All possible models from the independent variables (spindle speed, feed rate and depth of cut) were formed using the statistical analysis software (Minitab, 18V). The best model is the one with the highest values of (R-sq) and (R) and the lowest standard deviation, consisting of the fewest number of variables. Thus, the best possible model from the set of independent variables affecting the dependent variable was obtained. The regression equations resulting from the software in terms of un-coded factors are as follows:

$$\mathrm{Ra} = 2.2687 - 0.3030\,\mathrm{N} + 0.2860\,\mathrm{f} - 0.1970\,\mathrm{a} - 0.3468\,\mathrm{N}^2 - 0.0318\,\mathrm{f}^2 + 0.6432\,\mathrm{a}^2 - 0.0413\,\mathrm{N}*\mathrm{f} + 0.0112\,\mathrm{N}*\mathrm{a} + 0.0888\,\mathrm{f}*\mathrm{a} \quad (5)$$

$$\mathrm{MRR} = 5516.5 + 1926.5\,\mathrm{N} + 1908.1\,\mathrm{f} + 1865.3\,\mathrm{a} + 276\,\mathrm{N}^2 - 0\,\mathrm{f}^2 - 15\,\mathrm{a}^2 + 641.8\,\mathrm{N}*\mathrm{f} + 627.7\,\mathrm{N}*\mathrm{a} + 627.7\,\mathrm{f}*\mathrm{a} \quad (6)$$

Following experimental execution and model fitting, the predictive accuracy and adequacy of the established regression equations were rigorously evaluated using Fisher's variance ratio test (F-test) and Analysis of Variance (ANOVA). The ANOVA results for both response models are detailed in Table 4 and Table 5, respectively. Furthermore, model validity and statistical assumptions were verified through residual analysis, including tests for homoscedasticity (constant variance), independence, and normality of the residual distributions, as illustrated in Figure 6 and Figure 7.

The ANOVA results showed that the regression models are significant, as the F-test value for the surface roughness model was 20.86 and for the MRR model was 349.93. The P-values equal to 0.000, which are less than the significance level (5%), indicate that the models are important and significant. The linear and quadratic factors (N, f, a, N^2, a^2) were highly significant for the surface roughness model, and the linear factors and their interactions (N, f, a, Nf, Na, f*a) were highly significant for the MRR model. This means that there is a significant effect of the independent variables on the response variables. It is noteworthy that non-significant model terms should be excluded from the regression equations to improve them. The analysis also showed that the Adjusted R^2 values are very high for both models, indicating that the independent variables (spindle speed, feed rate and depth of cut) explain approximately 90.3% of the variance in surface roughness, with the remaining 9.7% possibly due to other factors like random error. They also explain approximately 99.1% of the variance in MRR, with the remaining 0.9% attributable to other factors including random error. The multicollinearity test (VIF - Variance Inflation

Factor) showed that the VIF value was 1.000 for the significant variables in both models, which is less than 3, indicating no linear multicollinearity problem among the model variables.

Table (4): (ANOVA) for Surface Roughness (Ra).

Term	Coef.	DOF	Adj-SS	F-Value	T-Value	P-Value	VIF
Regression	-	-	-	20.86	-	0.000	-
Constant	2.2687	-	-	-	48.46	0.000	-
N	-0.3030	1	0.91809	49.49	-7.04	0.000	1.00
f	0.2860	1	0.81796	44.10	6.64	0.000	1.00
a	-0.1970	1	0.38809	20.92	-4.57	0.001	1.00
N^2	-0.3468	1	0.33078	17.83	-4.22	0.002	1.82
f^2	-0.0318	1	0.00278	0.15	-0.39	0.707	1.82
a^2	0.6432	1	1.13763	61.33	7.83	0.000	1.82
N*f	-0.0413	1	0.01361	0.73	-0.86	0.412	1.00
N*a	0.0112	1	0.00101	0.05	0.23	0.820	1.00
f*a	0.0888	1	0.06301	3.40	1.84	0.095	1.00
Error	-	10	0.18549	-	-	-	-
Total	-	19	3.66718	-	-	-	-
R-Sq			94.94%				
R-Sq(adj)			90.39%				

Table (5): (ANOVA) for Material Removal Rate (MRR).

Term	Coef.	DOF	Adj-SS	F-Value	T-Value	P-Value	VIF
Regression	-	-	-	350.24	-	0.000	-
Constant	5516.5	-	-	-	-	0.000	-
N	1926.5	1	37114142	989.15	31.45	0.000	1.00
f	1908.1	1	36409036	970.36	31.15	0.000	1.00
a	1865.3	1	34793844	927.31	30.45	0.000	1.00
N^2	276	1	208792	5.56	2.36	0.040	1.82
f^2	-0	1	0	0.00	-0.00	0.998	1.82
a^2	-15	1	648	0.02	-0.13	0.898	1.82
N*f	641.8	1	3295422	87.83	9.37	0.000	1.00
N*a	627.7	1	3152550	84.02	9.17	0.000	1.00
f*a	627.7	1	3152550	84.02	9.17	0.000	1.00
Error	-	10	375212	-	-	-	-
Total	-	19	118647758	-	-	-	-
R-Sq			99.68%				
R-Sq(adj)			99.40%				

Figures (6) and (7) demonstrate the accuracy and efficiency of the regression models. The residuals are normally distributed (Normality) and evenly scattered around zero at all points of the independent variables, indicating that both models have good predictive accuracy for surface roughness and material removal rate. The figures also show that the relationship between the residuals and the independent variables appears as randomly scattered points in both negative and positive directions, with no specific patterns or clear curves, indicating that the residuals are homogeneous and that both models have high accuracy in randomly predicting the response outputs. Furthermore, the figures show that the relationship between the residuals and the data order displays residuals independently without following any increasing, decreasing, or repeating cyclical pattern, indicating that the residuals have a random pattern.

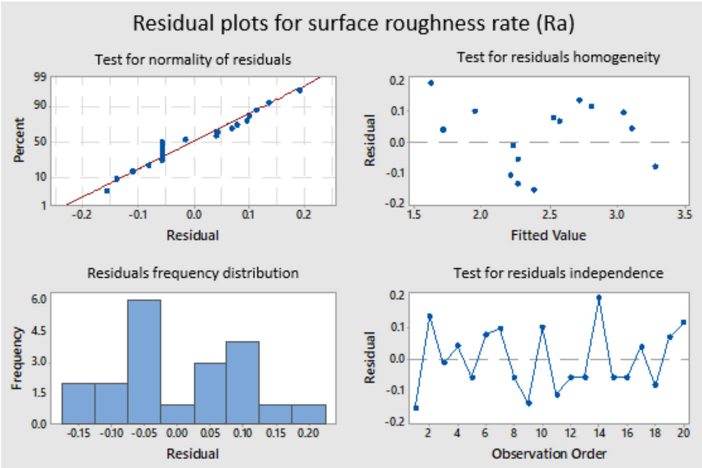

Figure (6): Residual Plots for Surface Roughness (Ra).

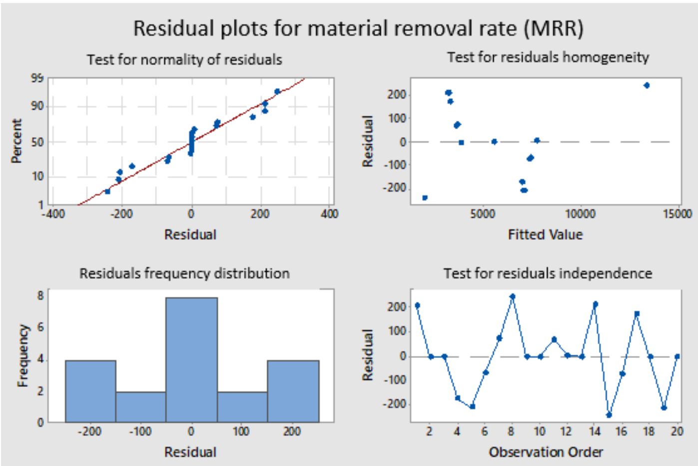

Figure (7): Residual Plots for Material Removal Rate (MRR).

Based on the above, it can be inferred that all analytical tests for the regression models confirm their accuracy and efficiency. Therefore, these models can be confidently used to predict the response outputs in the turning process of low-carbon steel alloy (AISI 1018).

B. Discussion of Factor Interaction Effects on Responses (3D Surface Plots)

1. Interaction Effect of Depth of Cut and Rotational Speed on Surface Roughness

Figure 8 shows that surface roughness (Ra) increased at both low and high depths of cut (a = 0.4 mm and 0.8 mm), while reaching a minimum at the intermediate level (a = 0.6 mm), particularly at high rotational speeds (N = 1120 rpm).

As noted by Hakuma et al[11], and Ben Aissa et al[12], low depths of cut cause material rubbing and plowing rather than effective shearing, leading to a degraded surface finish. Conversely, high depths of cut increase cutting forces and induce chatter, which negatively impacts surface finish—especially at lower rotational speeds (N = 560 rpm).

2. Interaction Effect of Depth of Cut and Feed Rate on Surface Roughness

Figure 9 shows that the relationship between surface roughness and feed rate is direct; surface roughness increases as the feed rate increases. This is due to increased cutting force and tool-work piece vibration, leading to higher surface roughness. Additionally, the increased temperature generated during cutting reduces tool life and increases surface roughness. When the cutting speed increases, the contact time between the work piece surface and the tool surface decreases, reducing tool vibration on the work piece surface and thus reducing surface roughness. It was also observed that the best surface roughness was obtained at medium values of depth of cut and low values of feed rate, as mentioned earlier in the effect of the depth of cut and spindle speed interaction.

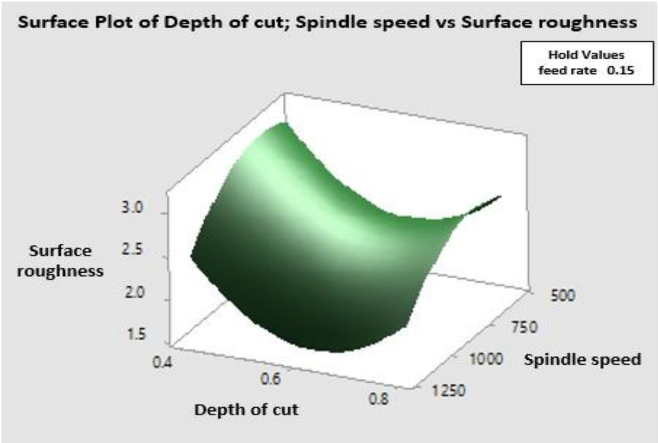

Figure (8): Effect of the interaction between Depth of Cut and Spindle Speed on Surface Roughness.

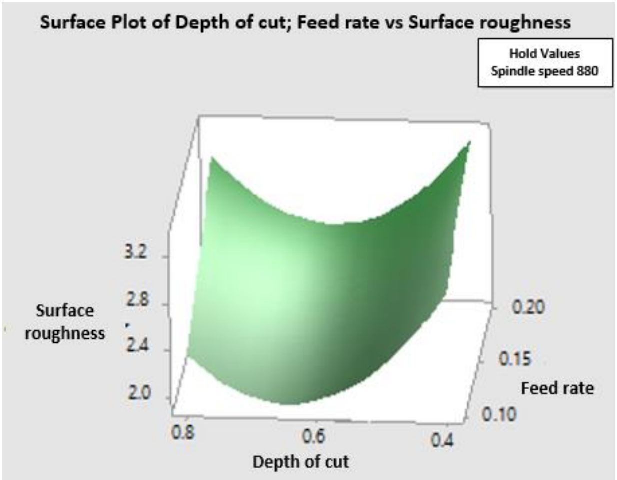

Figure (9): Effect of the interaction between Depth of Cut and Feed Rate on Surface Roughness.

3. Interaction Effect of Feed Rate and Rotational Speed on Surface Roughness

Figure 10 demonstrates that surface roughness decreases as feed rates are reduced. This occurs because higher feed rates result in more material contact with the cutting tool, thereby increasing cutting forces. These elevated forces cause vibrations that lead to increased surface roughness. Additionally, high feed rates elevate cutting temperatures, accelerating tool wear and consequently producing undesirable surface roughness.

Figure 10 also indicates that surface roughness decreases with increasing spindle speed. This phenomenon can be attributed to the fact that higher spindle speeds increase the shear angle value, resulting in a narrower

Furthermore, since the turned sample (low-carbon steel alloy) exhibits high ductility, it possesses a high coefficient of friction. During the initial stages of machining, this high coefficient of friction induces the Built-Up-Edge (BUE) phenomenon on the cutting tool surface and potentially on the tool tip.

4. Interaction Effect of Depth of Cut and Feed Rate on Material Removal Rate (MRR)

Figure 11 shows that the highest Material Removal Rate (MRR) was achieved at the maximum levels of depth of cut (a = 0.8 mm) and feed rate (f = 0.20 mm/rev), whereas the lowest MRR occurred at their minimum levels. Depth of cut exhibited the dominant influence on MRR. Overall, both parameters demonstrate a direct proportional relationship with MRR.

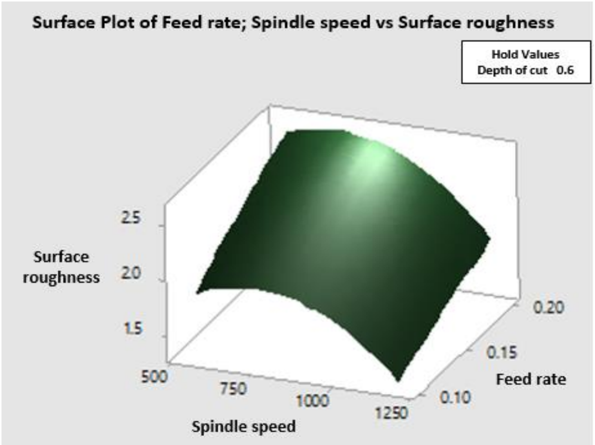

Figure (10): Effect of the interaction between Feed Rate and Spindle Speed on Surface Roughness.

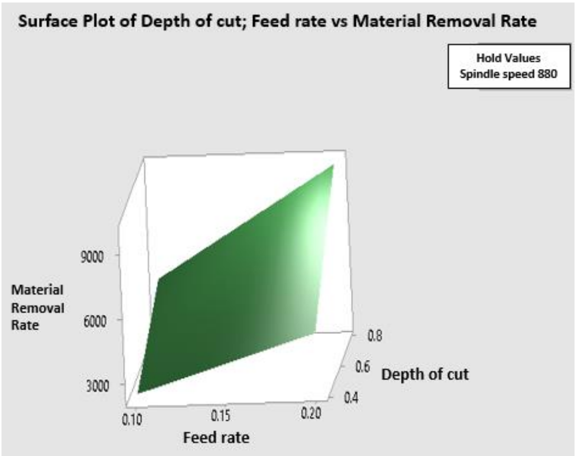

Figure (11): Effect of the interaction between Depth of Cut and Feed Rate on Material Removal Rate.

5. Interaction Effect of Feed Rate and Rotational Speed on Material Removal Rate (MRR)

Figure 12 shows that the highest MRR was at the high values of feed rate and spindle speed (0.2 mm/rev & 1120 rpm) and the lowest MRR was at the low values of feed rate and spindle speed. However, feed rate has a greater influence on MRR compared to spindle speed. A direct proportionality between these two factors and MRR is also evident.

6. Interaction Effect of Depth of Cut and Rotational Speed on Material Removal Rate (MRR)

Figure 13 shows that the highest MRR was at the high values of depth of cut (0.8 mm) and spindle speed (1120 Rev/min) and the lowest MRR was at the low values of depth of cut and spindle speed. However, depth of cut has the greater influence on MRR. A direct proportionality between these two factors and MRR is also evident.

C. Multi-Response Optimization and Confirmation Experiments

Using the Desirability Function Approach (DFA) in Minitab, the cutting conditions were optimized to simultaneously minimize surface roughness (Ra) and maximize Material Removal Rate (MRR).

1. Multi-Objective Optimization

The optimization yielded the optimal global machining parameters: a rotational speed (N) of 1120 rpm, a feed rate (f) of 0.20 mm/rev, and a depth of cut (a) of 0.6788 mm. This combination concurrently achieved a minimum surface roughness (Ra) of 1.8934 µm and a maximum Material Removal Rate (MRR) of 11459 mm³/min, as illustrated in Figure 14.

2. Single-Response Optimization

Single-response desirability analysis predicted optimal parameters for each objective independently:

- Surface Roughness Minimization:

A minimum Ra of 1.3131 µm is achieved at N = 1120 rpm, f = 0.10 mm/rev, and a = 0.6424 mm Figure 15.

- Material Removal Rate Maximization:

A maximum MRR of 13373.6 mm³/min is achieved at N = 1120 rpm, f = 0.20 mm/rev, and a = 0.80 mm Figure 16.

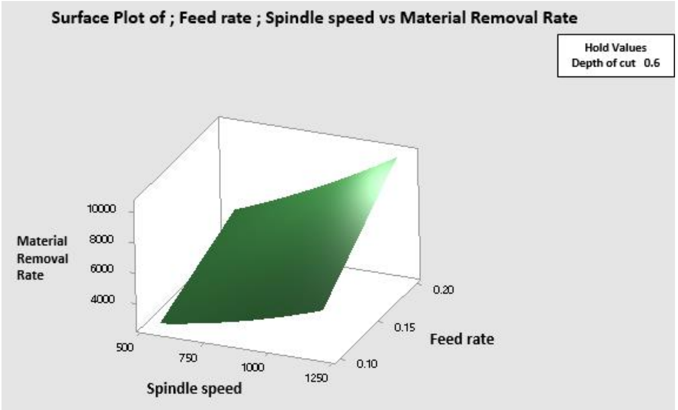

Figure (12): Effect of the interaction between Feed Rate and Spindle Speed on Material Removal Rate.

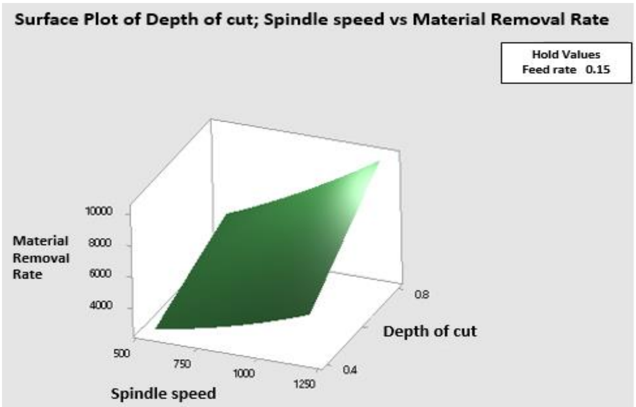

Figure (13): Effect of the interaction between Depth of Cut and Spindle Speed on Material Removal Rate.

C. Confirmation Experiments

Validation experiments were conducted under the software-predicted optimal machining conditions to verify model accuracy. Table 6 presents the experimentally measured response values versus the predicted results. The percentage error between the experimental and predicted responses ranged from 1.7% to 5.5%. This minor variation confirms the reliability and predictive capability of the established models.

Conclusion

This study demonstrated that spindle speed, feed rate, and depth of cut are the primary factors influencing both surface roughness and material removal rate. Their effects are not only individual but also interdependent through interaction effects. The results showed that increasing spindle speed and feed rate enhanced material removal rate, while higher feed rate and depth of cut increased surface roughness due to elevated cutting forces and vibrations. The regression models developed in this study exhibited high reliability, with adjusted R^2 values of 90.3% for surface roughness and 99.1% for material removal rate, indicating that these models capture most of the process variability. Residual analysis confirmed that the models satisfy fundamental statistical assumptions, thereby validating their predictive capability. Using the desirability function approach enabled simultaneous optimization of both responses. The optimal cutting parameters were determined as: Spindle speed: 1120 rpm Feed rate: 0.2 mm/rev Depth of cut: 0.6788 mm. These parameters achieved minimum surface roughness (1.8934 µm) and maximum material removal rate (11,459 mm³/min). Confirmation experiments validated the predictions with error margins of only 1.7–5.5%. The integrated methodology combining Response Surface Methodology with desirability-based optimization provides a practical and versatile framework for optimizing various machining processes.

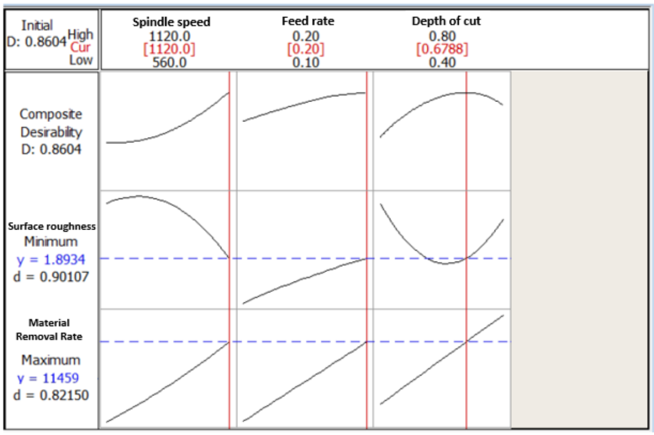

Figure (14): Target desirability plot for optimizing (Ra) and (MRR).

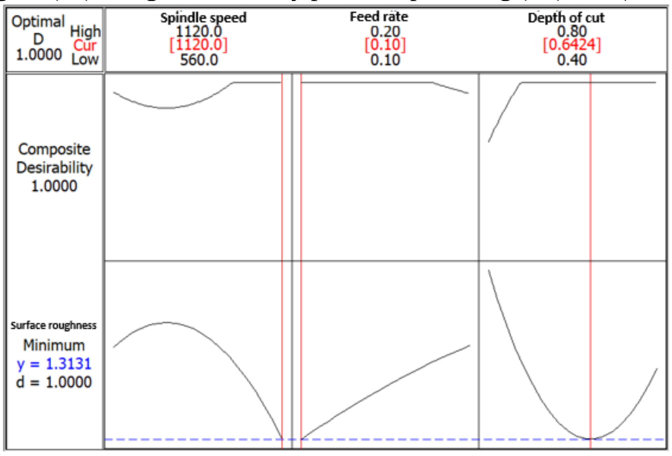

Figure (15): Individual desirability plot for minimizing (Ra).

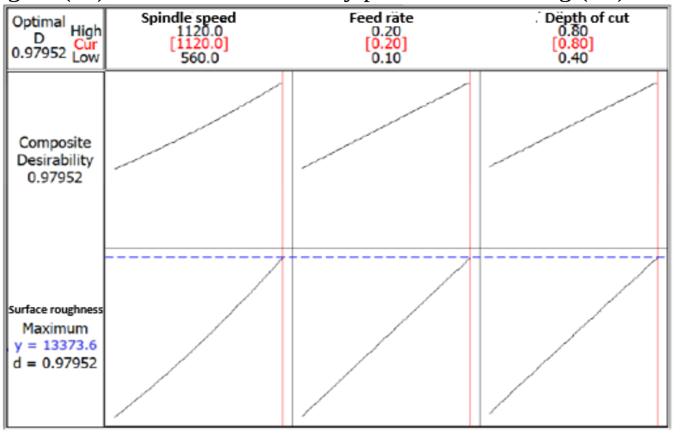

Figure (16): Individual desirability plot for maximizing (MRR).

Table (6): Predicted and actual response values and the error percentage between them.

Response Type	Desirability Function Required	Optimal Combination of Cutting Parameters			Predicted Response Value	Actual Response Value	Error %
		Spindle Speed N (rpm)	Feed Rate f (mm/rev)	Depth of Cut a (mm)			
Ra MRR	Optimal / Target	1120	0.20	0.6788	1.8934 11459	1.85 10997.19	2.345 4.199
Ra	Minimize	1120	0.10	0.6424	1.3131	1.39	5.532
MRR	Maximize	1120	0.20	0.80	13373.6	13617.05	1.787

Recommendations

- The optimized cutting parameters obtained in this study should be implemented in industrial practice, as they can enhance productivity and reduce overall costs.
- To further strengthen predictive accuracy, future research is encouraged to include additional factors such as tool geometry, tool material, and the influence of cutting fluids.
- Advanced computational techniques, particularly artificial neural networks and modern optimization algorithms, should be integrated with conventional statistical approaches to provide more powerful and reliable tools for process modeling and optimization.

Conflict of interest statement: "The authors declare no conflicts of interest."
Author Contributions: "All authors have made a substantial, direct, and intellectual contribution to the work and approved it for publication."
Funding: "This research received no external funding."
Data Availability Statement: "No data were used to support this study."

Conflict of interest statement: "The authors declare no conflicts of interest."
Author Contributions: "All authors have made a substantial, direct, and intellectual contribution to the work and approved it for publication."
Funding: "This research received no external funding."
Data Availability Statement: "No data were used to support this study."

References

[1] A. T. Abbas, A. A. Al-Abduljabbar, M. M. El Rayes, F. Benyahia, I. H. Abdelgaliel, and A. J. M. Elkaseer, "Multi-objective optimization of performance indicators in turning of AISI 1045 under dry cutting conditions," vol. 13, no. 1, p. 96, 2023.

[2] M .A. Khan *et al.*, "Multi-objective optimization of turning titanium-based alloy Ti-6Al-4V under dry, wet, and cryogenic conditions using gray relational analysis (GRA)," vol. 106, no. 9, pp. 3897-3911, 2020.

[3] Y. Touggui, S. Belhadi, S.-E. Mechraoui, A .Uysal, M. A. Yallese, and M. J. S. A. S. Temmar, "Multi-objective optimization of turning parameters for targeting surface roughness and maximizing material removal rate in dry turning of AISI 316L with PVD-coated cermet insert," vol. 2, no. 8, p. 1360.2020 ,

[4] S. S. Warsi, M. H. Agha, R. Ahmad, S. H. I. Jaffery, and M. J. T. I. J. o. A. M. T. Khan, "Sustainable turning using multi-objective optimization: a study of Al 6061 T6 at high cutting speeds," vol. 100, no. 1, pp. 843-855, 2019.

[5] R. Roy *et al.*, "Multi-response optimization of surface grinding process parameters of AISI 4140 alloy steel using response surface methodology and desirability function under dry and wet conditions," vol. 12, no. 1, p. 104, 2022.

[6] X. Zhang, X. Li, H. Wang, and T .J. A. i. M. E. Zhang, "Multi-objective optimization of machining parameters during milling of carbon-fiber-reinforced polyetheretherketone composites using grey relational analysis," vol. 12, no. 10, p. 1687814020966232, 2020.

[7] N. Malekjani and S. M. Jafari, "Food process modeling and optimization by response surface methodology (RSM)," in *Mathematical and statistical applications in food engineering*: CRC Press, 2020, pp. 181-203.

[8] NIST/SEMATECH. (April .(2012 ,*e-Handbook of Statistical Methods*. Available: https://www.itl.nist.gov/div898/handbook/index.htm

[9] N. R. Costa and J. J. J. o. C. Lourenço, "Multiresponse problems: Desirability and other optimization approaches," vol. 30, no. 12, pp. 702-714, 2016.

[10] R. Amdoun *et al.*, "The desirability optimization methodology; a tool to predict two antagonist responses in biotechnological systems: case of biomass growth and hyoscyamine content in elicited datura starmonium hairy roots," vol. 16, no. 1, p. e1339, 2018

[11] م. ع. حكومه, م. م. ب. عيسى, ه. ع. السويحلي, غ. إ. إبراهيم, and ب. ص. ي. J. ا. ا. ل. ا. والتقنية, "دراسة عوامل القطع المثلى لخشونة السطح في عملية الخراطة الطولية لعينة من سبيكة الألومينيوم باستخدام طريقة تاقوتشي: عملية الخراطة," vol. 6, no. 5، مجلة الجامعة الأسمرية, 2021, pp. 408-395.

[12] M. M. B. Isa, H. A. Aswihli, and A. J .ا .ا .م.Alkhwaji, "Experimental investigation of cutting parameters effect on surface roughness during wet and dry turning of low carbon steel material," vol. 17, pp. 10-16, 2021.

تحسين الأداء متعدد الاستجابات في عملية خراطة سبائك الفولاذ منخفض الكربون باستخدام منهجية سطح الاستجابة ونهج دالة الرغبة

مصطفى عمر حكومة[1]، سالم عطية بلعيد[1]، أبوبكر عبدالحميد حمّير[2]، بالنور معتوق[3]، عبدالناصر محمد اشتيوي[4]

[1]الجامعة الأسمرية الإسلامية، قسم الهندسة الميكانيكية والصناعية، ليبيا

[2]المعهد العالي للتقنيات الهندسية، قسم الهندسة الميكانيكية، ليبيا
[3]جامعة المرقب، قسم الهندسة الميكانيكية، ليبيا
[4]الهيئة الليبية للبحث العلمي، ليبيا

الملخص

في هذه الدراسة، تم تطبيق منهجية سطح الاستجابة (RSM) مع نهج دالة الرغبة (DFA) لتحديد القيم المثلى لمتغيرات القطع (سرعة القطع، معدل التغذية، وعمق القطع) بهدف تقليل خشونة السطح إلى الحد الأدنى وتعظيم معدل إزالة المعدن الى الحد الاقصى (MRR). ولتنفيذ التجارب بكفاءة، استخدم تصميم مركب مركزي متمركز على وجه المكعب (FCCD). كما تم تطوير نماذج رياضية من الدرجة الثانية لكل من معدل إزالة المعدن وخشونة السطح (Ra) بالاعتماد على النتائج التجريبية. وقد جرى التحقق من صلاحية هذه النماذج باستخدام اختبار (F- tests) بينما تم تقييم كفاءتها من خلال تحليل التباين (ANOVA) للاستجابات المستهدفة. بعد ذلك، جرى تحسين متغيرات القطع بالاعتماد على النماذج التنبؤية المطورة عبر RSM، في حين تم تحسين الاستجابات المتعددة من خلال نهج الاستحسان القائم على دالة الرغبة DFA أظهرت النتائج أن القيم المثلى لمتغيرات القطع التي نتج عنها أقل خشونة سطحية (1.8934 ميكرومتر) وأعلى معدل إزالة للمعدن (11,459 ملم / دقيقة)، تحققت عند سرعة دوران مقدارها 1120 دورة / دقيقة، ومعدل تغذية قدره 0.20 ملم / دورة، وعمق قطع يساوي 0.6788 ملم. وتؤكد هذه النتائج فعالية المنهجية المقترحة في تحسين أداء التشغيل لسبائك الفولاذ منخفض الكربون.

استلمت الورقة بتاريخ 2026/07/17، وقبلت بتاريخ 2026/08/26، ونشرت بتاريخ 2026/08/29

الكلمات المفتاحية: تحليل التباين، خشونة السطح، سطح الاستجابة، عوامل القطع، معدل إزالة المعدن.